Relationship between sprite streamer behavior and lightning-driven electric fields

Jingbo Li[1] and Steven Cummer[1]

[1] The lightning-driven electric fields not only initiate sprite streamers at high altitudes but also control their propagation to lower altitudes until termination. Thus, the relationship between sprite streamer behavior and their causative lightning-driven ambient electric field can reveal the internal microphysics during sprite development. In this work, we combined the measurements of broadband electromagnetic radiation from sprite-producing lightning, high-speed video of sprite optical emissions acquired at 5,000–10,000 frames per second, and numerical simulations to infer the background lightning-driven electric fields during the full extent of downward streamer propagation. For four sprites analyzed, all with positive polarity downward streamers, the observed streamers all terminate at locations where the ambient electric field is approximately $0.05\,E_k$, independent of the altitude where this field is reached. For two sprites with significant horizontal extent, the points of streamer termination closely follow the spatial contour of the $E = 0.05\,E_k$ surface, further confirming the consistency of this termination background field for positive sprite streamers. The positive streamers also begin their significant deceleration where the background field drops below 0.12–$0.24\,E_k$. These measured termination field (E_{ter}) and deceleration field (E_{dec}) are consistent with previous laboratory experiments of positive streamer stopping field and critical field to sustain stable propagation. These results connect sprite streamer behavior with the lightning-driven background electric fields and can be a step to further constrain the existing model of streamer propagation in the mesosphere.

1. Introduction

[2] Sprites are produced by lightning discharges and are observed in the altitude range of ∼40–90 km above thunderstorms [*Sentman*, 1995]. Previous measurements of sprite optical emissions have revealed its fine structure by telescope [*Gerken et al.*, 2000; *Gerken and Inan*, 2002] and by high-speed videos [*Stanley et al.*, 1999; *Stenbaek-Nielsen et al.*, 2000; *Cummer et al.*, 2006; *McHarg et al.*, 2007]. Sprite streamers have been interpreted in terms of positive and negative streamer coronas similar to the small-scale streamers existing at high atmospheric pressures [*Pasko et al.*, 1998; *Pasko*, 2007; *Liu and Pasko*, 2004]. The initiation of sprite streamers is caused by conventional air breakdown of lightning-driven electric fields [*Pasko et al.*, 1997]. After initiation, streamers continue to propagate because of the lightning-driven background electric fields. Thus, understanding the relationship between lightning-driven background electric fields and the streamers behavior can help

reveal the internal microphysics and chemical process inside sprites streamers.

[3] Laboratory experiments have been conducted with different setups to study the propagation behaviors of corona streamers, such as their diameters and velocities [*Briels et al.*, 2008a, 2008b], critical ambient electric field to sustain stable propagation [*Phelps*, 1971; *Phelps and Griffiths*, 1976; *Allen and Ghaffar*, 1995], and streamer terminating fields [*Nasser et al.*, 1968]. However, with a few exceptions [*Opaits et al.*, 2010], most of the laboratory experiments were conducted in a homogenous medium with high air atmospheric pressure. Thus, it is not always easy to scale the laboratory experimental results to sprite streamers, which propagate in inhomogeneous medium with varying air density.

[4] After first being applied by *Stanley et al.* [1999], high-speed video has been proven useful to study the sprite streamer propagation properties, such as their morphologies [*Cummer et al.*, 2006], optical emission rates [*Stenbaek-Nielsen et al.*, 2007], velocities and acceleration rates [*Moudry et al.*, 2002; *McHarg et al.*, 2007; *Li and Cummer*, 2009]. *McHarg et al.* [2007] first measured the sprite streamer velocities and acceleration rate at their initiation stage, while *Li and Cummer* [2009] measured the sprite streamer velocities, and associated acceleration and deceleration during their entire altitude extent.

[1]Department of Electrical and Computer Engineering, Duke University, Durham, North Carolina, USA.

[5] Measurements from multianode photometer essentially show the same results [*McHarg et al.*, 2002] as high-speed video. The connections between these streamer behaviors and the involving physical and chemical processes have been extensively studied by numerical modeling. *Raizer et al.* [1998] modeled the streamer propagation in an inhomogeneous atmosphere by treating the lightning source as an electric dipole. By including the internal chemical and photoionization processes, *Liu and Pasko* [2004, 2005] have developed a model to simulate the propagation of streamers in constant normalized electric fields (E/E_k) at different altitudes. *Luque and Ebert* [2009, 2010] have simulated streamer propagation properties in a varying air density.

[6] Although all these previous studies have revealed many important features of sprite streamers, the connection between sprite streamer features and the lightning-driven background electric fields have not been measured yet. Moreover, the numerical modeling results can be sensitive to the input parameters, including these ambient fields. All the existing models have assumed constant and spatially uniform electric fields [*Luque and Ebert*, 2010], constant normalized electric fields [*Liu and Pasko*, 2004, 2005; *Liu*, 2010], or electric fields computed with the electrostatic dipole approximation [*Raizer et al.*, 1998; *Luque and Ebert*, 2009] as the background fields. These approximations may provide valid results of streamer propagation in a small range and short time period, for example, at the stage of sprite initiation [*Liu et al.*, 2009]. However, they are not accurate enough to predict the streamer properties in the entire sprite altitude extent, especially the lower-altitude portion, where streamers propagate in weaker normalized electric fields and occupy a substantial part of the entire sprite volume. Measurements can both define this behavior and help guide future modeling improvements.

[7] In this work, we combine the high-speed video images and simultaneously measured lightning-radiated magnetic fields to measure the relationship between electric fields and streamer behavior. We present measurement-derived background electric field altitude profiles in real sprites that can be used in simulations to include realistic physical fields instead of the simplified uniform or dipole fields used in most existing simulations. For four sprites analyzed, we find that the positive streamers in different sprites all terminate at the location where ambient electric field is approximately 0.05 E_k. This termination field (E_{ter}) is also observed in the horizontally varying termination altitude for two sprites with many elements and thus significant horizontal extent. The dependence of streamer termination altitude on ambient field is generally consistent with the stopping field measured in lab experiments [*Nasser et al.*, 1968]. We find that most of the positive streamer deceleration occurred when the ambient electric field falls below 0.12–0.24 E_k. This deceleration field (E_{dec}) is not significantly different from previous laboratory experiments [*Phelps*, 1971; *Allen and Ghaffar*, 1995] and simulation results [*Liu and Pasko*, 2006]. Collectively, these measurements provide important data on sprite dynamics and can be used to constrain existing models.

2. Instrumentation and Methods

[8] During a measurement campaign in 2005, we simultaneously measured high-altitude sprite optical emissions and broadband electromagnetic radiation from sprite parent lightning at the Yucca Ridge Field Station (40.702°N, −105.031°E) near Fort Collins, Colorado, United States. The magnetic sensors, a pair of coils with flat bandwidth from <1 Hz to 30 kHz built by Quasar Federal Systems, yielded signals continuously sampled at 100 kHz. Additionally, data from the National Lightning Detection Network (NLDN) provided each return stroke location. The lightning location and two orthogonal horizontal measurements of the magnetic field from each pair of coils enabled us to derive the azimuthal magnetic field (the magnetic field in the azimuthal ($\hat{\phi}$) direction defined by a cylindrical coordinate system with the origin at the lightning location). A high-speed camera, capable of recording high-speed images up to 10,000 frames per second, was used to record the sprite optical emissions. The field of view was more than 10° and covered the entire altitude range for sprites that occurred a few hundred kilometers away. All the systems were synchronized with GPS and the absolute time accuracy was verified to be better than 20 μs. More details about these instruments have been presented in several previous papers [*Cummer et al.*, 2006; *Li et al.*, 2008; *Li and Cummer*, 2009].

[9] On 13 August 2005, the high-speed camera captured seven sprites produced by two thunderstorms about 300 and 450 km away from the observation site. The resulting spatial resolution is about 140 m/pixel for the sprite images (640 × 480) during the first thunderstorm (300 km) and about 260 m/pixel for the sprite images during the second one (450 km). We estimated the streamer tip locations from high-speed videos and background star field [*Li and Cummer*, 2009]. The unknown radial separation between sprites and their parent lightning discharges (a few tens of kilometers [*Wescott et al.*, 2001]) contributes an overall altitude uncertainty of approximately ±3 km for every ±10 km change in radial offset for lightning 300–400 km away from the observation site. To track an individual streamer head, we define the edge of the streamer as the point where the luminosity is at least 2 times the background noise level. The termination altitude is determined at the location where the minimum luminosity (2 times the noise level) appears at the same location in successive image.

[10] The lightning-driven electric fields are estimated by applying a method introduced by *Hu et al.* [2007] and *Li et al.* [2008], which combines a deconvolution technique [*Cummer and Inan*, 1997; *Cummer*, 2003] and finite difference time domain (FDTD) simulations [*Hu et al.*, 2006]. In this work, we have improved the original deconvolution technique to estimate the lightning source current in a broader bandwidth and described in detail below.

2.1. Lightning Source Waveform Estimation

[11] The original deconvolution technique extracts lightning source in the frequency band of 0–1.5 kHz. This technique has been proven to be useful in estimating the total charge moment change for lightning and sprite currents. Although the 1.5 kHz upper frequency bound does not affect the computed total charge moment change, it may not be able to reflect the timescale of the true lightning source current waveform, which includes a fast risetime and thus a much wider frequency band. In this work, we modified the original deconvolution technique to extract the lightning
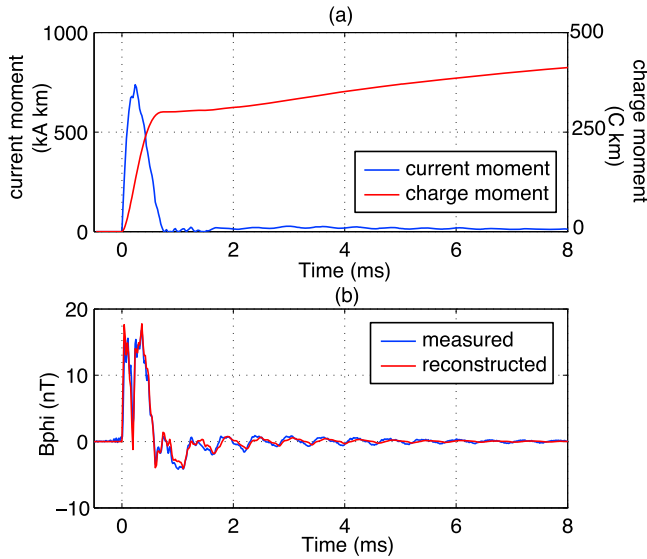
Figure 1. An example of full bandwidth lightning source current moment waveform. (a) Extracted lightning source current moment waveform in a frequency band of 0–25 kHz. (b) Comparison of measured and reconstructed lightning sferics at the observation site in time domain.

source current in the frequency band of 0–25 kHz. Since the remotely measured lightning-radiated magnetic field is the convolution of the lightning source current and the impulse response of Earth-ionosphere waveguide, extracting a broadband lightning current source requires that both the measured data and the impulse response should cover the above frequency range. To achieve this, we apply a very narrow pulse and fine step size in the FDTD model to ensure the desired frequency band of the Earth-ionosphere impulse response. The lightning source current is then extracted with a linear regulation algorithm and enforced that the radiated sferics from this source perfectly matched the measurements.

[12] Figure 1a shows an example of the extracted lightning source current moment and total charge moment change. With this lightning source, we reconstructed the lightning sferics at the observation site and compare it with the measured magnetic field (Figure 1b). The good agreement in the time domain waveform demonstrates that the extracted source reliably represented the detailed features in the higher frequencies, such as the fast risetime about 100 μs. It should be mentioned that, with the aforementioned approach, the fastest risetime that can be resolved is about 30 μs. This limitation is mainly imposed by the upper cutoff (30 kHz) of the magnetic field sensor. For example, a 10 μs risetime will be degraded to 30 μs after passing through the sensor.

2.2. High-Altitude Field Prediction

[13] We then apply the full-band current source as an input to the FDTD model. The full-wave FDTD model computes electric fields as a function of both time and location above the thundercloud. Nonlinear effects, like heating, attachment, and ionization processes have been incorporated in this model using the parameterization described by *Pasko et al.* [1997]. These nonlinear effects critically affect the

computed electric fields at regions with high electron densities [*Li et al.*, 2008], which we now demonstrate. With the same current source shown in Figure 1a, we compare the vertical electric field directly above the lightning discharge computed from three different models: the full-wave FDTD model with nonlinear effects, the FDTD model without nonlinear effects, and a simple purely electrostatic dipole model. Assuming a conducting ionosphere is at 90 km altitude, the total electric field produced by a dipole and its image is [*Raizer et al.*, 1998]

$$E(h) = \frac{Qdl}{\pi\epsilon_0 h^3}\left[1 + \left(\frac{h}{180-h}\right)^3\right]\exp\left[-\frac{t}{\tau(h)}\right] \quad (1)$$

$$\tau(h) = \frac{\epsilon_0}{\sigma(h)}, \quad (2)$$

where Qdl is the total charge moment change in C km, h is the altitude in km, t is the time in s, ϵ_0 is the permittivity of vacuum, and $\sigma(h)$ is the regular ionosphere conductivity at night, which is computed from a two-parameter exponential electron density profile [*Han and Cummer*, 2010].

[14] For convenience, we again show the same lightning current source in Figure 2a with three time instances at 0.7, 2, and 6 ms. The total charge moment change at these times are 300, 312, and 386 C km. Figure 2b shows the normalized
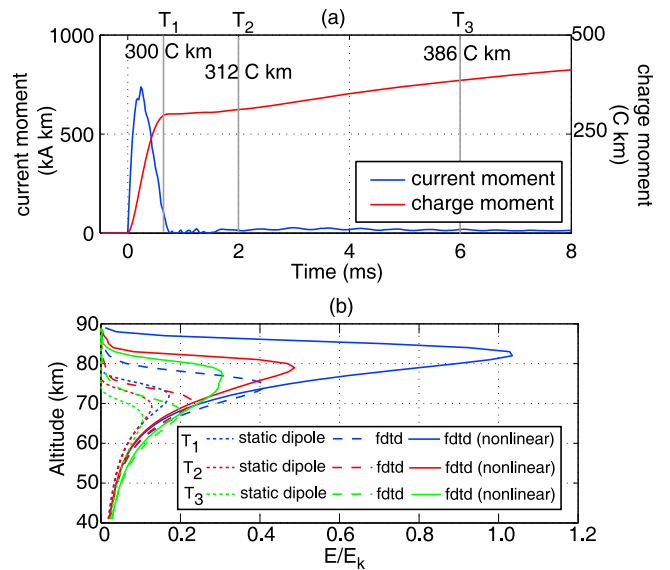
Figure 2. Comparison between electric fields directly above the lightning discharge computed from (1) full-wave finite difference time domain (FDTD) model with nonlinear effects of attachment, heating, and ionization, (2) full-wave FDTD model without the nonlinear effects, and (3) an electrostatic dipole model. (a) Lightning source current moment and total charge moment change. At the three time instances, $T_1 = 0.7$ ms, $T_2 = 2$ ms, and $T_3 = 6$ ms, the total charge moment changes are 300, 312, and 386 C km, respectively. (b) Normalized electric fields at 40–90 km altitude computed from the three models.
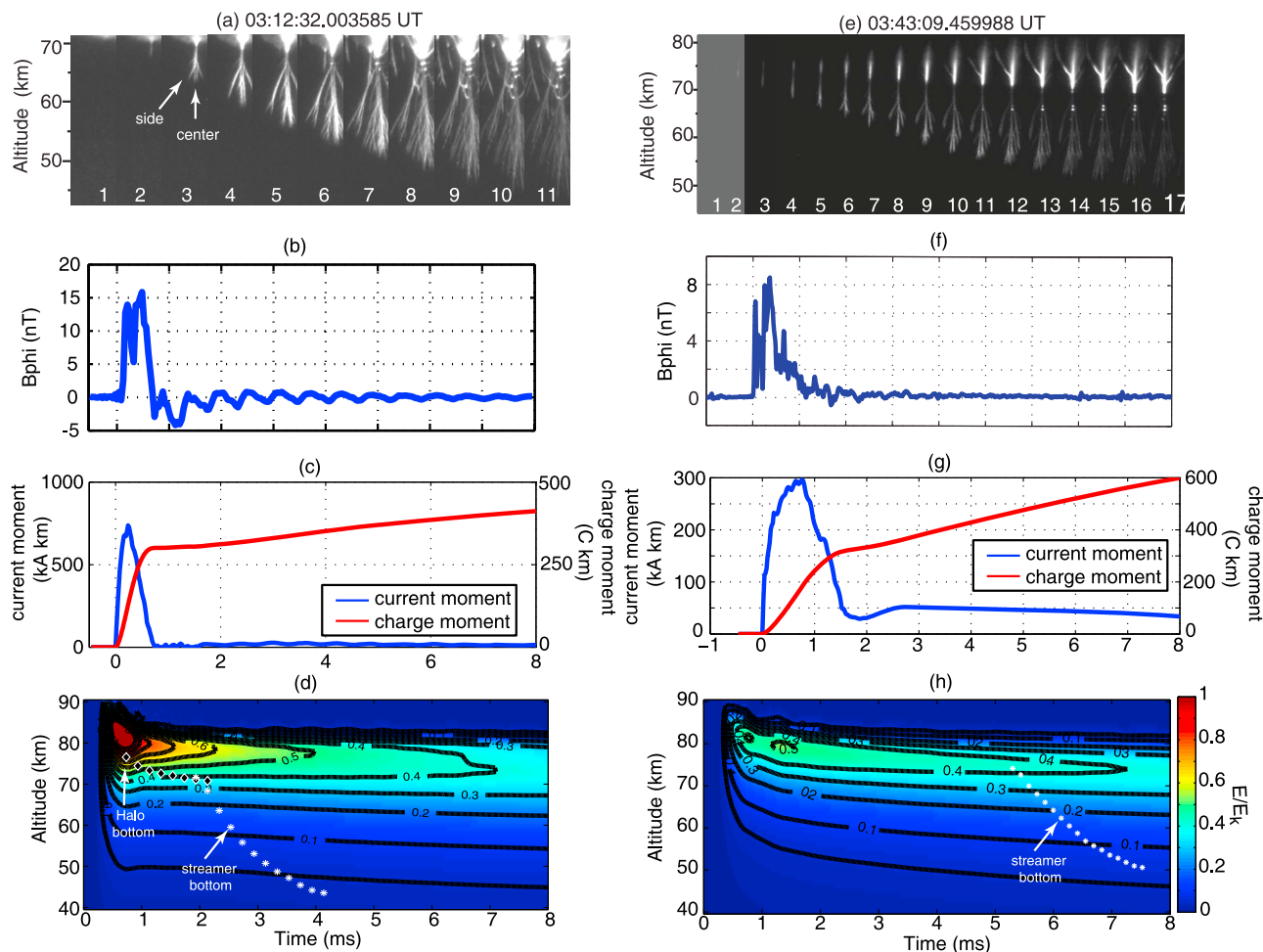
Figure 3. Example of a typical sprite that occurred on 13 August 2005, 03:12 UT. (a) High-speed images recorded at 5000 fps (or Δt = 0.2 ms). (b) Measured magnetic field in azimuthal direction. (c) Retrieved full-band lightning source current moment and total charge moment waveform. (d) Normalized electric fields above the lightning discharge computed from the FDTD model. The black diamonds represent the bottom location of the sprite halo. The white asterisks represent the locations of the downward streamer tip. (e–h) The same quantities for another sprite detected at 03:43 UT.

E field (E/E_k) above the lightning discharge in 40–90 km altitude range computed from the three models. At altitudes above 60 km, there is a significant difference between the three results. The FDTD results with nonlinear effects have the highest fields and the electrostatic dipole model have the lowest fields. For example, at T_1 = 0.7 ms, the normalized electric field exceeds E_k at ~80 km altitude from the FDTD results with nonlinear effects. Without the nonlinear effects, the field is about 0.4 E_k at ~75 km altitude. This indicates the nonlinear effects not only increase the maximum normalized electric field but also push it to a higher altitude. Without the nonlinear effects and with an electrostatic approximation, the maximum normalized electric field computed from the dipole model is only 0.2 E_k at around ~70 km altitude. Below 60 km altitude, the fields from different models are comparable because of a much lower electron density and weaker nonlinear effects. The scenarios are similar at the other two time instances. This comparison shows that excluding the nonlinear effects or using the purely electrostatic dipole

model can cause significant underestimation of the lightning-driven electric fields, especially at the high-altitude portion with higher electron densities.

3. Measured Streamer Velocity and Background Electric Field

[15] With the aforementioned approach, we next show the relationship between sprite streamer propagation properties and lightning-driven ambient electric fields.

3.1. Examples of Positive Downward Sprite Streamers

[16] Here we present the electric field during positive downward streamer propagation in the entire altitude range from initiation to termination measured during two sprites. Figures 3a–3d show a sprite whose streamers initiated from a bright halo, which occurred on 13 August 2005 at 03:12 UT. Figure 3a shows the high-speed images recorded at 5000 fps (or Δt = 0.2 ms). At 0.7 ms after the lightning discharge, a

Table 1. Lightning Charge Moment Change at the Time of Sprite Initiation, the Range of Streamer Propagation Altitude, and Normalized Electric Fields for the Four Sprites Analyzed

Event Time (UT)	Charge Moment Change (C km)	Streamer Tip Altitude (km)	E/E_k
03:12	312	73–44	0.40 − 0.04
03:25	335	72–42	0.46 − 0.04
03:43	310	74–51	0.42 − 0.06
04:14	302	70–49	0.32 − 0.05

sprite halo becomes visible. Approximately 2 ms after the return stroke, sprite streamers initiate from the bottom of the halo at about 70 km altitude (image 1). Streamer velocity was tracked by measuring the location of the bottom tip of the central streamer group. In the third image of Figure 3a, the downward streamer branches into development in center and side directions. Although this branching may affect the streamer velocity, it is hard to quantify this effect in this work. In cases where complicated branching prevents the tracking of individual streamers, we measure the velocity from the lowest-altitude streamer, which usually appears at the center of the sprite. The downward streamer tip travels to the termination altitude of ~45 km in the next 2 ms. From the extracted lightning current moment waveform shown in Figure 3c, the total charge moment change is 300 C km at the time of halo initiation (0.7 ms) and 312 C km at the time of sprite initiation (2 ms). This charge moment change falls in the range of typical shortly delayed sprites [*Hu et al.*, 2007; *Li et al.*, 2008]. With the lightning source current, we inferred the lightning-driven (time- and space-varying) electric fields directly above the lightning discharge. For our examples in this work, all the sprites occurred within a few milliseconds after the lightning discharge. Considering these short time delays, we assumed that charges are removed from a 2 km radius disk in the thundercloud in our FDTD model.

[17] In Figure 3d, the color intensity represents the inferred normalized electric field from 40 km altitude to 90 km altitude. At 0.7 ms after the lightning discharge, the normalized electric fields exceed the local air breakdown field at altitudes above 80 km. This high-field region cannot initiate streamer structures because of the high local electron density and thus the fast electrical relaxation time. Instead, a sprite halo is produced by the high field and propagates downward as the high-altitude fields relax. The bottom trace of the sprite halo is shown with black diamonds. At ~2 ms, a sprite initiates from the bottom of the sprite halo. The time and altitude of the central streamer tip are plotted as the white asterisks. At the streamer initiation altitude, the normalized electric field is close to 0.4. As the streamer tip moves to lower altitudes, this normalized electric field decreases. At the termination altitude of 45 km, this normalized electric field is about 0.04. It is clear that after the initiation stage, the downward streamer travels from the region of stronger normalized electric fields to weaker normalized electric fields.

[18] Figures 3e–3h show another example that occurred on the same day. The high-speed images were recorded at 7200 fps. The sprite initiated at about 76 km altitude. At the time of initiation, the bottom tip of the downward streamer is about 74 km altitude. The normalized electric

field at this time and location is about 0.4. As the streamer tip propagates to lower altitudes, the normalized electric field decreases. At the termination altitude around 50 km, the normalized electric field is about 0.06. These features are similar to the first example at 03:12 UT. It is worth to mention that when sprite streamers traveling to the lower region, the normalized electric field becomes less sensitive to altitudes. This effect can be seen in Figures 3d and 3f, where the contour lines of the normalized electric field are sparse at lower altitudes.

3.2. Summary of Measurements

[19] For the four events analyzed, we summarized the streamer properties and normalized electric fields in Table 1, which shows the sprite-producing lightning charge moment change at the time of sprite initiation, altitude range of downward streamer tip, and the range of normalized electric fields at the streamer tip locations.

[20] In our previous work [*Li and Cummer*, 2009], we reported the altitude, propagation velocity, and acceleration/deceleration rate for these four sprites. Here we connect these observations with the lightning-driven background electric fields. Figure 4 (top) shows streamer tip velocity versus altitudes. All streamers initiated between 70 and 80 km altitude and accelerated to their maximum velocity in less than 5 km from their apparent initiation altitude. It should be mentioned that our high-speed images may not provide enough time resolution to reveal the details at this stage because of a big field of view to include the entire sprite altitude extent. After that, the streamer velocity decreases with decreasing altitude before reaching the termination altitude between 45 and 55 km. The scenario for the event at 03:43 UT is slightly different. After reaching the maximum velocity, the streamer has a close-to-constant velocity of 1.4×10^7 m/s to 60 km altitude. After that, the streamer velocity quickly decays to zero. Although a general acceleration then deceleration trend is detected in Figure 4 (top), the streamer velocity shows a big difference at each altitude. Furthermore, streamers in different sprites terminate at different altitudes with a variation about 9 km. This poor alignment indicates that the streamer velocity and termination location do not depend on altitudes.

[21] We next plot the streamer velocity versus the normalized ambient electric fields in Figure 4 (bottom). At the time of initiation, the normalized electric fields vary from 0.32 to 0.46 E_k, which is consistent with previous studies [*Hu et al.*, 2007; *Li et al.*, 2008; *Gamerota et al.*, 2011]. As streamers travel downward, both the electric fields and the velocity decrease. Comparing with Figure 4 (top), the velocities align much better with normalized electric fields instead of altitudes. For the four streamers, although they initiate at locations with different ambient electric fields and terminate at different altitudes, the ambient electric fields are all close to 0.05 E_k at their termination. We name this as the termination field (E_{ter}). As we mentioned earlier, part of the reason that we see a large variation in the termination altitude but small range in the termination field is caused by the slow change of normalized electric field at lower altitudes around 40 km. For example, a normalized electric field from 0.04 to 0.06 corresponds to an altitude change about 5 km. However, this is still less than the 9 km variation shown in different events. Thus, the small range of E_{ter} indicates the
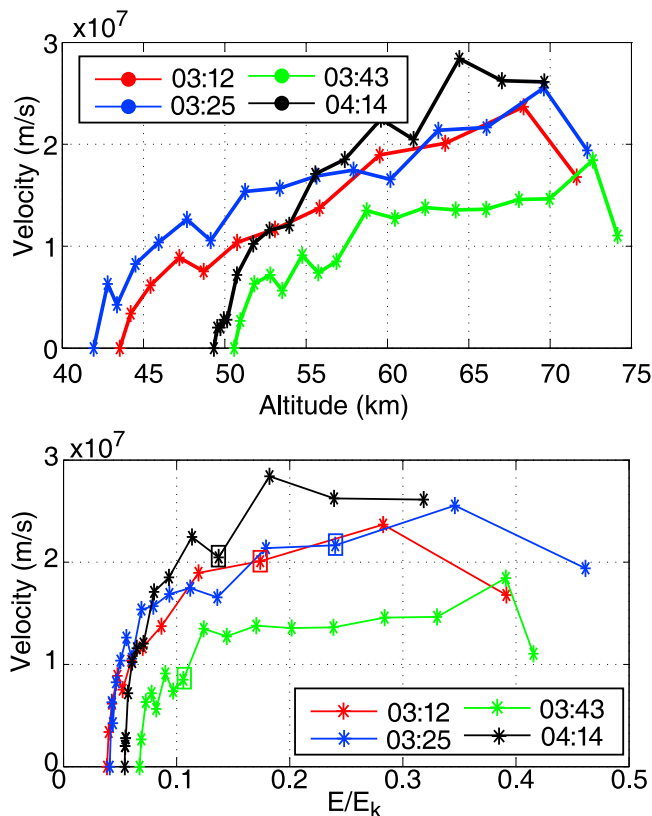
Figure 4. (top) Downward streamer tip propagation velocity versus altitude for four different sprites. (bottom) Streamer propagation velocity versus normalized electric fields. The squares represent locations where significant deceleration starts.

dependence of streamer termination on the lightning-driven background electric field at ~0.05 E_k. The experimental result in Figure 4 (bottom) indicates that this termination field does not depend on the streamer initiation field and peak velocity. For example, the 03:43 event and 04:14 show big variations in their initiation field (0.42 E_k versus 0.32 E_k) and peak velocity (1.8 × 10^7 versus 2.8 × 10^7 m/s). However, they both terminate at the location where the ambient electric field is ~0.05 E_k. Besides this termination field, Figure 4 (bottom) also allows us to measure the field where significant deceleration occurs (E_{dec}). For the events that occurred at 03:12, 03:25, and 04:14 UT, in which the velocities have an acceleration then deceleration process, the first deceleration occurred when the normalized fields were 0.17, 0.24, and 0.14. For the event at 03:43 UT, which contains an acceleration–constant-deceleration process, although the first deceleration occurs after the maximum velocity at 0.32 E_k, significant deceleration occurs below 0.12 E_k after the constant velocity. Thus, significant deceleration starts between 0.12 and 0.24 E_k for the four events, with majority of the deceleration below 0.2 E_k.

3.3. Spatial Distribution of Streamer Termination Location and Fields

[22] Above measurements of E_{ter} from different sprite events show the dependence of streamer termination location on lightning-driven electric field. Next, we examine this

feature in sprites containing multiple sprite elements. For the sprites that occurred on 03:25 and 04:14 UT, the sprite contains multiple elements at the stage of full development. We inferred the lightning-driven electric fields at the bottom streamer tip for each of the sprite elements and show them in Figure 5. Figure 5a (left) shows the high-speed image for the sprite event at 03:25 UT. At 4.7 ms after the lightning discharge, the sprite is fully developed. This complicated event contains many single elements at different locations. We labeled the termination locations of downward streamer tips for 5 identifiable elements. If we assume the brightest element is directly above the lightning discharge, the relative distances of other elements can be directly read from the high-speed image. It should be mentioned that we have also assumed that all these elements are in the same 2-D plane as the high-speed image. In reality, these sprite elements occurred in 3-D space. Projecting a 3-D sprite into a 2-D plane results in an underestimation of the relative distance between each sprite elements to the center. However, this uncertainty is hard to quantify without triangulation of sprites. We then inferred the lightning-driven background fields at the same instance as shown in Figure 5a (right). The termination location of different elements is also labeled on this field map. At all these locations, the termination fields (E_{ter}) are close to the lowest contour line at 0.05 E_k except the right most one, which is much dimmer and may occur far away from the center element. A similar phenomenon is observed in the event at 04:14 UT, as shown in Figure 5b. The high-speed image shows five sprite elements at the stage of full development, which is 3.2 ms after the lightning discharge. In the field map, the E_{ter} at five termination locations are all close to contour line at 0.05 E_k. In these examples, although the different elements occurred at different locations and terminated at different altitudes, the termination field is close to 0.05 E_k. Thus, it further confirms the dependence of streamer termination location on the background electric field. In both examples above, the termination field for the side elements is slightly higher than that of the center elements. Part of the reason could be the underestimation of their relative distance to the center. In real 3-D space, these side elements could occur at a farther distance and thus smaller termination field.

4. Comparison With Previous Laboratory Experiments and Simulations

[23] We next compare the measured threshold quantities with previous laboratory measurements conducted at high atmospheric pressure. We first compare the measured E_{dec} with the critical field to sustain positive streamer propagation reported by *Phelps* [1971]. In this laboratory experiment, the positive streamer propagates in an uniform ambient field between two plane electrodes. They reported a critical field between 630 and 740 kV/m (0.2–0.23 E_k) depending on the temperature and humidity. *Allen and Ghaffar* [1995] conducted a similar experiment and reported a minimum threshold of 440 kV/m (0.14 E_k). Simulation results from *Liu and Pasko* [2006] shown a critical field about 0.16 E_k. Although sprite streamers propagate in nonuniform electric fields and inhomogeneous medium in our measurement, our measured E_{dec} is not significantly different with previously reported critical field to sustain stable propagation for positive
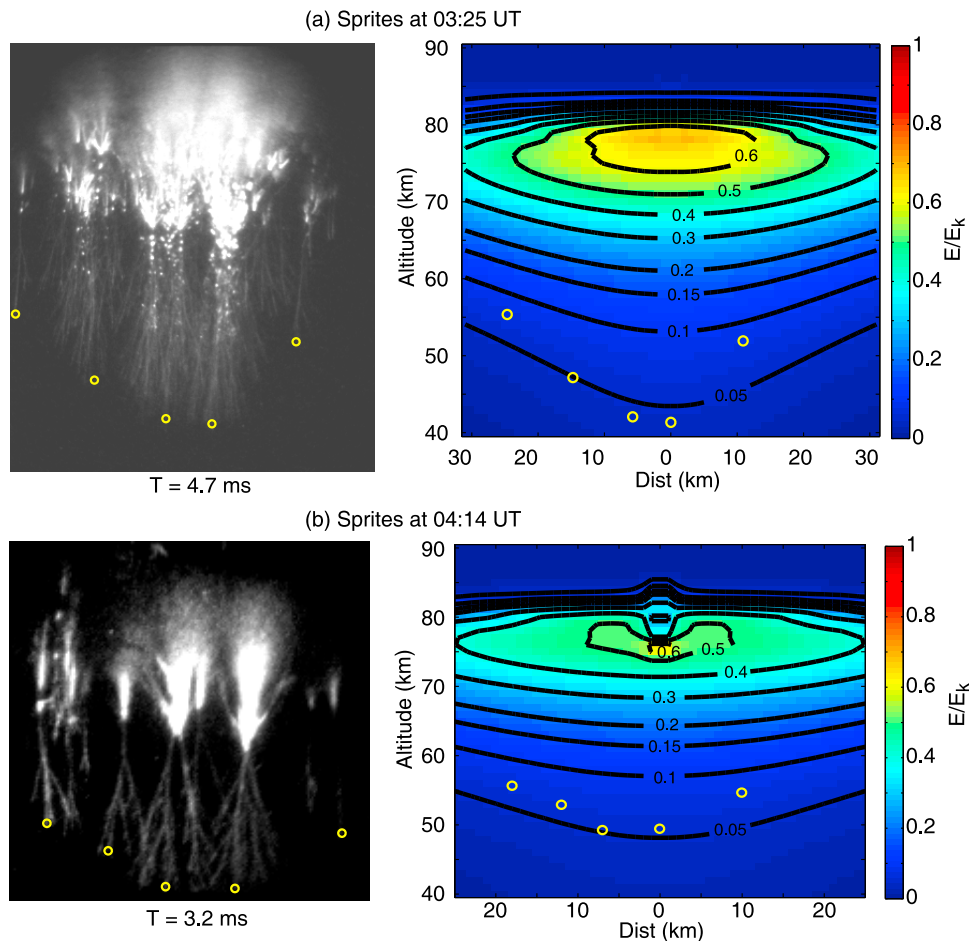
Figure 5. (a) High-speed image and inferred lightning-driven ambient electric fields for a sprite that occurred at 03:25 UT. (left) High-speed images of different sprite elements fully developed at 4.7 ms after the parent lightning. (right) Normalized electric fields at the same instance. (b) High-speed image and inferred lightning-driven ambient electric fields for a sprite that occurred at 04:14 UT. (left) High-speed images of different sprite elements fully developed at 3.2 ms after the parent lightning. (right) Normalized electric fields at the same instance. The yellow circles represent the termination location of each sprite element.

streamers. We next compare the measured E_{ter} with the stopping field reported by *Nasser et al.* [1968]. In this experiment, the positive streamer propagate in a nonuniform electric field between a point anode and a plane cathode. They reported that positive streamers stop at locations at 600 V/m (0.02 E_k), which is lower than the measured E_{ter} of 0.05 E_k. Part of the difference could be caused by the dimness of sprite streamers when approaching the termination location. Thus, the actual termination altitude is lower than appeared on high-speed images. However, a normalized field of 0.02 E_k is at about or below 30 km altitude for events analyzed. Up to now, no sprite event has been reported to propagate down to that altitude. More interestingly, *Nasser et al.* [1968, p. 3707] stated "the streamers tend to stop whenever the applied field drops below the field regardless of gap spacing or streamer location." This is extremely consistent with our measurements that E_{ter} are all close to 0.05 E_k regardless of the different termination locations for different sprites or different elements in complicated sprite clusters. The good consistency between our measurements and previous laboratory experiments validates our approach and results. It also implies that the lightning-driven ambient electric field controls the streamer propagation in the same way as the electric fields in the laboratory experiments at high atmospheric pressure.

[24] We also compare our results with recent numerical simulations reported by *Luque and Ebert* [2010]. They simulated the propagation velocity of downward positive streamers with a constant electric field of 40 V/m in the region of 55–90 km altitude. Although the simulations results also show an acceleration-deceleration process, the velocity starts to drop at ambient electric field below E_k. During the time period of 1–2 ms after the streamer initiation, the simulation results shown a slow decrease of streamer velocity from 0.84 to 0.56×10^7 m/s and the corresponding ambient electric field varies from 0.83 to 0.32 E_k [see *Luque and Ebert*, 2010, Figure 3]. Clearly these results do not agree with our measured streamer velocity and inferred ambient fields. Thus, a constant ambient electric field cannot truly represent the real situation.

5. Conclusions

[25] In this work, we report the lightning-driven background electric field during the propagation of positive

downward streamers by combining high time resolution measurement of lightning-radiated magnetic fields, sprite optical emissions, and numerical simulations. With the measured lightning-radiated magnetic fields, we first extract lightning source current waveforms with a resolvable rise-time as short as 30 μs. Then we applied this current source to a 2-D FDTD model, which includes the nonlinear effects of heating and ionization. By comparing with an electrostatic dipole model, our results show that excluding the nonlinear effects or using the electrostatic dipole model will cause significant underestimation of the lightning-driven background fields especially at higher altitudes greater than 60 km. By inferring the ambient field at downward streamer tips during the entire sprite altitude range, we found the events generally experienced an acceleration then deceleration process and two threshold field quantities at deceleration (E_{dec}) and termination (E_{ter}) are measured. The deceleration field (E_{dec}) varies from 0.12 to 0.24 E_k, below which the velocity of positive downward streamers significantly drops. Although the four analyzed sprite events terminated at different altitudes, the measured termination fields (E_{ter}) are all close to 0.05 E_k. Thus, it indicates the strong dependence of streamer termination on the ambient electric fields. This dependence is further confirmed by examining the E_{ter} for different elements in two complicated sprites. In these two sprites with significant horizontal extent, the E_{ter} for each sprite element is close to the 0.05 E_k contour line independent of their locations. These results are consistent with previous laboratory experiments conducted at high atmospheric pressure.

[26] At the current stage of sprite streamer modeling, various models have applied the constant electric fields, constant normalized fields, or electric fields computed with static dipole approximation as the ambient field. Our results show that none of the above approximations can truly reflect the lightning-driven background fields in the entire sprite altitude range. The purely electrostatic approximation can cause significant underestimation of the lightning fields above 60 km altitude. Assuming constant or constant normalized ambient electric fields may provide valid results for streamer propagation in a small range and short time period, for example, at the initiation stage of streamer propagation [*Liu et al.*, 2009]. However, these assumptions are not adequate to predict the streamer properties in the entire sprite altitude range. In this work, we show the weak and varying lightning-driven ambient electric fields from the initiation up to the termination altitude. These measurements provide important data input to further constrain the existing streamer models and show the detailed electric field environment in which sprite streamers propagate.

[28]   Robert Lysak thanks the reviewers for their assistance in evaluating this paper.

References

Allen, N. L., and A. Ghaffar (1995), The conditions required for the propagation of a cathode-directed positive streamer in air, *J. Phys. D Appl. Phys.*, *28*, 331–337.

Briels, T. M. P., E. M. van Veldhuizen, and U. Ebert (2008a), Streamers in air and nitrogen of varying density: Experiments on similarity laws, *J. Phys. D Appl. Phys.*, *41*, 234008, doi:10.1088/0022-3727/41/23/234008.

Briels, T. M. P., J. Kos, G. J. J. Winands, E. M. van Veldhuizen, and U. Ebert (2008b), Positive and negative streamers in ambient air: Measuring diameter, velocity and dissipated energy, *J. Phys. D Appl. Phys.*, *41*, 234004, doi:10.1088/0022-3727/41/23/234004.

Cummer, S. A. (2003), Current moment in sprite-producing lightning, *J. Atmos. Sol. Terr. Phys.*, *65*, 499–508.

Cummer, S. A., and U. S. Inan (1997), Measurement of charge transfer in sprite-producing lightning using ELF radio atmospherics, *Geophys. Res. Lett.*, *24*, 1731–1734.

Cummer, S. A., N. Jaugey, J. Li, W. A. Lyons, T. E. Nelson, and E. A. Gerken (2006), Submillisecond imaging of sprite development and structure, *Geophys. Res. Lett.*, *33*, L04104, doi:10.1029/2005GL024969.

Gamerota, W. R., S. A. Cummer, J. Li, H. C. Stenbaek-Nielsen, R. K. Haaland, and M. G. McHarg (2011), Comparison of sprite initiation altitudes between observations and models, *J. Geophys. Res.*, *116*, A02317, doi:10.1029/2010JA016095.

Gerken, E. A., and U. S. Inan (2002), A survey of streamer and diffuse glow dynamics observed in sprites using telescopic imagery, *J. Geophys. Res.*, *107*(A11), 1344, doi:10.1029/2002JA009248.

Gerken, E. A., U. S. Inan, and C. P. Barrington-Leigh (2000), Telescopic imaging of sprites, *Geophys. Res. Lett.*, *27*, 2637–2640.

Han, F., and S. A. Cummer (2010), Midlatitude nighttime D region ionosphere variability on hourly to monthly time scales, *J. Geophys. Res.*, *115*, A09323, doi:10.1029/2010JA015437.

Hu, W., S. A. Cummer, W. A. Lyons, and T. E. Nelson (2006), An FDTD model for low and high altitude lightning-generated EM fields, *IEEE Trans. Antennas Propag.*, *54*, 1513–1522.

Hu, W., S. A. Cummer, and W. A. Lyons (2007), Testing sprite initiation theory using lightning measurements and modeled electromagnetic fields, *J. Geophys. Res.*, *112*, D13115, doi:10.1029/2006JD007939.

Li, J., and S. A. Cummer (2009), Measurement of sprite streamer acceleration and deceleration, *Geophys. Res. Lett.*, *36*, L10812, doi:10.1029/2009GL037581.

Li, J., S. A. Cummer, W. A. Lyons, and T. E. Nelson (2008), Coordinated analysis of delayed sprites with high-speed images and remote electromagnetic fields, *J. Geophys. Res.*, *113*, D20206, doi:10.1029/2008JD010008.

Liu, N. (2010), Model of sprite luminous trail caused by increasing streamer current, *Geophys. Res. Lett.*, *37*, L04102, doi:10.1029/2009GL042214.

Liu, N., and V. P. Pasko (2004), Effects of photoionization on propagation and branching of positive and negative streamers in sprites, *J. Geophys. Res.*, *109*, A04301, doi:10.1029/2003JA010064.

Liu, N., and V. P. Pasko (2005), Molecular nitrogen LBH band system far-UV emissions of sprite streamers, *Geophys. Res. Lett.*, *32*, L05104, doi:10.1029/2004GL022001.

Liu, N., and V. P. Pasko (2006), Effects of photoionization on similarity properties of streamers at various pressures in air, *J. Phys. D Appl. Phys.*, *39*, 327–334.

Liu, N. Y., V. P. Pasko, K. Adams, H. C. Stenbaek-Nielsen, and M. G. McHarg (2009), Comparison of acceleration, expansion, and brightness of sprite streamers obtained from modeling and high-speed video observations, *J. Geophys. Res.*, *114*, A00E03, doi:10.1029/2008JA013720.

Luque, A., and U. Ebert (2009), Emergence of sprite streamers from screening-ionization waves in the lower ionosphere, *Nat. Geosci.*, *2*, 757–760, doi:10.1038/NGE0662.

Luque, A., and U. Ebert (2010), Sprites in varying air density: Charge conservation, glowing negative trails and changing velocity, *Geophys. Res. Lett.*, *37*, L06806, doi:10.1029/2009GL041982.

McHarg, M. G., R. K. Haaland, D. Moudry, and H. C. Stenbaek-Nielsen (2002), Altitude-time development of sprites, *J. Geophys. Res.*, *107*(A11), 1364, doi:10.1029/2001JA000283.

McHarg, M. G., H. C. Stenbaek-Nielsen, and T. Kammae (2007), Observations of streamer formation in sprites, *Geophys. Res. Lett.*, *34*, L06804, doi:10.1029/2006GL027854.

Moudry, D. R., H. C. Stenbaek-Nielsen, D. D. Sentman, and E. M. Wescott (2002), Velocities of sprite tendrils, *Geophys. Res. Lett.*, *29*(20), 1992, doi:10.1029/2002GL015682.

Nasser, E., M. Heiszler, and M. Abou-Seada (1968), Field criterion for sustained streamer propagation, *J. Appl. Phys.*, *39*(8), 3707–3713.

Opaits, D. F., M. N. Shneider, P. J. Howard, R. B. Miles, and G. M. Milikh (2010), Study of streamers in gradient density air: Table top modeling of red sprites, *Geophys. Res. Lett.*, *37*, L14801, doi:10.1029/2010GL043996.

Pasko, V. P. (2007), Red sprite discharges in the atmosphere at high altitude: The molecular physics and the similarity with laboratory discharges, *Plasma Sources Sci. Technol.*, *16*, S13–S29.

Pasko, V. P., U. S. Inan, and T. F. Bell (1997), Sprite produced by quasi-electrostatic heating and ionization in the lower ionosphere, *J. Geophys. Res.*, *102*, 4529–4561.

Pasko, V., U. Inan, and T. Bell (1998), Spatial structure of sprites, *Geophys. Res. Lett.*, *25*, 2123–2126.

Phelps, C. T. (1971), Field-enhanced propagation of corona streamers, *J. Geophys. Res.*, *76*, 5799–5806.

Phelps, C. T., and R. F. Griffiths (1976), Dependence of positive corona streamer propagation on air pressure and water vapor content, *J. Appl. Phys.*, *47*(7), 2929–2934, doi:10.1063/1.323084.

Raizer, Y., G. Milikh, M. Shneider, and S. Novakovski (1998), Long streamer in the upper atmosphere above thundercloud, *J. Phys. D Appl. Phys.*, *31*(22), 3255–3264.

Sentman, D. D. (1995), Preliminary results from the Sprites94 aircraft campaign: 1. Red sprites, *Geophys. Res. Lett.*, *22*, 1205–1208.

Stanley, M. S., P. Krehbiel, M. Brook, C. Moore, W. Rison, and B. Abrahams (1999), High speed video of initial sprite development, *Geophys. Res. Lett.*, *26*, 3201–3204.

Stenbaek-Nielsen, H., D. R. Moudry, E. M. Wescott, D. D. Sentman, and F. T. S. Sabbas (2000), Sprites and possible mesospheric effect, *Geophys. Res. Lett.*, *27*, 3829–3832.

Stenbaek-Nielsen, H., M. G. McHarg, T. Kanmae, and D. D. Sentman (2007), Observed emission rates in sprite streamer heads, *Geophys. Res. Lett.*, *34*, L11105, doi:10.1029/2007GL029881.

Wescott, E. M., H. C. Stenbaek-Nielsen, D. D. Sentman, M. J. Heavner, D. R. Moudry, and F. T. S. Sabbas (2001), Triangulation of sprites, associated halos and their possible relation to causative lightning and micrometeors, *J. Geophys. Res.*, *106*, 10,467–10,477.

S. Cummer and J. Li, Department of Electrical and Computer Engineering, Duke University, 130 Hudson Hall, Durham, NC 27708, USA. (jingbo.li@duke.edu)